



Research Article

Received: March 17, 2025

Accepted: April 6, 2025

Published: April 29, 2025

ISSN 2658-5553

Multi screw type elements for weak soil reinforcement

Nurmukhametov, Renat Rustamovich ¹ 

¹ Peter the Great St. Petersburg Polytechnic University, 195251, Saint Petersburg, Russia;
nrenatkazan@gmail.com

Correspondence:* email nrenatkazan@gmail.com; contact phone [+79063209900](tel:+79063209900)

Keywords:

Weak soil; Vertical reinforcement; Soil reinforcement; FRP piles; Micropiles; Helical piles; Screw piles; Fiber reinforced plastic pipes; Multi-screw elements; Soil improvement

Abstract:

The object of research is weak soils reinforced with fiber-reinforced plastic pipes with helical screws of increasing diameters from bottom to top, installed in weak soils at defined spacing. The study aims to develop and validate a new predictive settlement calculation model for weak soils reinforced with fiber-reinforced plastic pipes with helical screws of increasing diameters from bottom to top, installed in weak soils at defined spacing. **Method.** Method is based on a comparative review of closest researches. The reinforced mass is treated as a composite structure in which the vertical elements and surrounding soil undergo joint and simultaneous deformation. An analytical settlement calculation model was formulated based on a newly introduced reinforcement factor, which accounts for the geometry and structural characteristics of the reinforcing elements. **Results.** To validate the model, five full-scale axial load tests were conducted on soils reinforced with elements of different configurations. At pressure 300 kPa settlement reductions of 63% (samples with two screws) and 72% (three screws) were achieved. Comparative analysis of the calculated settlements and experimental results demonstrated the accuracy and applicability of the proposed method.

1 Introduction

Weak soils are widely distributed globally, predominantly in areas with high water saturation. They are characterized by a low deformation modulus, typically below 10 MPa. Construction on such soils is risky not only due to significant settlements but also because of their unpredictability across different parts of a site, which can lead to inclination of superstructures [1], [2].

Conventional settlement calculation methods, which summarize vertical deflections by predicting compaction depth, often underestimate actual settlements. In some cases, discrepancies reach several times the calculated values, resulting in unacceptable design errors. These inaccuracies arise because conventional methods neglect the intermolecular structure of weak soils and the horizontal decompaction processes that contribute to settlement.

Construction on weak soils without special measures is difficult or even impossible. Improvement measures may target either soil parameters or structural modifications to reduce the impact of settlements. Structural measures include increasing rigidity (e.g., using belts or box foundations) or dividing buildings into rigid blocks that settle independently of each other. Soil modification is typically achieved by drainage, chemical or physical strengthening to form new intergranular bonds, or by incorporating rigid elements. While such inclusions do not alter intermolecular interactions, they increase the material's modulus of elasticity. Examples include piles, strengthening elements, and reinforcements.

Reinforcement refers to the creation of a composite soil–structure system by introducing rigid elements that provide boundary interaction with the soil. Initially, reinforcement was mainly applied in road and hydraulic engineering projects, where it enabled calculation of bearing capacity [3] and stability

Nurmukhametov R.

Multi screw type elements for weak soil reinforcement;
2025; *AlfaBuild*; **34** Article No 3404. doi: 10.57728/ALF.34.4



[4], [5]. Various models have been developed using limit equilibrium theory, finite element analysis [6,7], and other approaches [8–10].

Most commonly, soil reinforcement is horizontal [11], using fabrics, geonets, or bars [12]. Studies [13] investigated reinforcement mats made of bamboo [14], wood, or straw, emphasizing their low cost and environmental safety. Other research [15], [16] focused on the durability, adhesion, and deformability of FRP elements (bars, piles) in soil environments.

Mustakimov V.R. proposed a classification of reinforcement that includes vertical, inclined, cross-shaped, and intermittent horizontal forms. Historically, weak soils were reinforced with sand and lime piles to improve the deformation modulus. Comparative analyses by Grishina A.S. [17], [18] show the diversity of methods for enhancing soil rigidity. Sabri M.M.S. [19], [20] emphasized that the choice of method depends on soil properties, economic efficiency, and project requirements.

Jet grouting is widely used [21]. Here, self-hardening mortars penetrate into weak soils, compacting the mass and forming vertical reinforcement elements [22]. A similar approach was investigated by Sabri M.M.S. [23], [24], who proposed strengthening weak soils with self-expanding polyurethane injection.

Existing settlement calculation methods for reinforced soils remain limited. Zhang D.J.Y. and Polischuk A.I. introduced the concept of a "cylindrical shear surface" to describe the joint action of screw-shaped extensions and surrounding soil where interlocking increases shear resistance. Mirsayapov I.T. and Popov A.O. [25], [26] suggested using an equivalent deformation modulus that accounts for the length and density of reinforcement within a soil volume.

$$S_{a3} = \frac{\beta}{E_{zp,\mu}^{\text{экв}}} \cdot \sum_{i=1}^n \sigma_{zp}^{a3,cp} \Delta_i, \quad (1)$$

$$E_{zp,\mu}^{\text{экв}} = \left[\frac{E_{zp} (A_{zp} - A_{a3}) (\gamma_{\varepsilon i} + \gamma_{\zeta i})}{A_{zp}} + \frac{E_{a3} A_{a3} (\gamma_{\varepsilon i} - \gamma_{\zeta i})}{A_{zp}} \right] \cdot \gamma_n, \quad (2)$$

$$E_{zp,m}^{\text{экв}} = \left[\frac{E_{zp} (A_{zp} - A_{a3}) (\gamma_{\varepsilon i} + \gamma_{\zeta i})}{A_{zp}} + \frac{(\gamma_{\varepsilon i} - \gamma_{\zeta i}) \sum f_i u_i l_i^{a3}}{A_{zp}} \cdot \frac{n}{A_{zp}} \right] \cdot \gamma_n. \quad (3)$$

Bartolomey A.A. developed factors for evaluating shear and base contact of vertical structures. Popsuenko K.I. observed that reinforced soils are often modeled as transversely isotropic in current codes, where settlements are calculated from reinforcement-to-soil volume ratios without considering surface interactions, leading to conservative designs and material overuse. Zahmatkesh A. [27] also proposed using equivalent elastic modulus, comparing results with those of Poorooshab and Meyerhof [28].

Studies [29,30] highlight the growing interest in helical screws and shear extensions, which are primarily used in anchors and micropiles. Research has focused on the mobilization of soil resistance and the influence of screw geometry on bearing capacity. However, most existing studies investigate steel elements or those with steel central shafts.

Overall, research has primarily examined reinforced soils, composite materials, and screw structures separately. A comprehensive review [31], [32], [33] confirms the lack of fundamental and applied studies on the combined system of weak soil reinforced with multi-helical vertical elements.

Therefore, existing methods are insufficient for settlement calculations in weak soils reinforced with multi-helical vertical elements. The present study addresses this gap by developing a reinforcement method using such elements and proposing a corresponding settlement prediction model.

The object of research is weak soils reinforced with fiber-reinforced plastic pipes with helical screws of increasing diameters from bottom to top, installed in weak soils at defined spacing. The subject of research is deformability parameters of reinforced weak soil. The study aims to propose and validate the method of weak soils strengthening and settlements assessment.

The research goals are

1. To propose a new scheme of weak soils strengthening by installation of vertical FRP reinforcing elements with screws.
2. To develop a settlement calculation method.
3. To validate the proposed method by full-scale tests.

Nurmukhametov R.

Multi screw type elements for weak soil reinforcement;
2025; *AlfaBuild*; 34 Article No 3404. doi: 10.57728/ALF.34.4

2 Materials and Methods

2.1 Model

The investigated method involves installing vertical reinforcing elements into weak soil to increase its deformation modulus. This effect is achieved when the reinforcing elements and the surrounding soil act together as a composite material with unified deformation characteristics. Consequently, the required installation depth is shallower than the depth of the underlying strong soil, which has a higher bearing capacity.

The depth of reinforcement depends on the applied surface load and the thickness of the compacted soil layer, H_{hc} (Figure 1). The method involves installing multiple vertical elements in the weak soil, with spacing determined by the calculation procedure described herein.

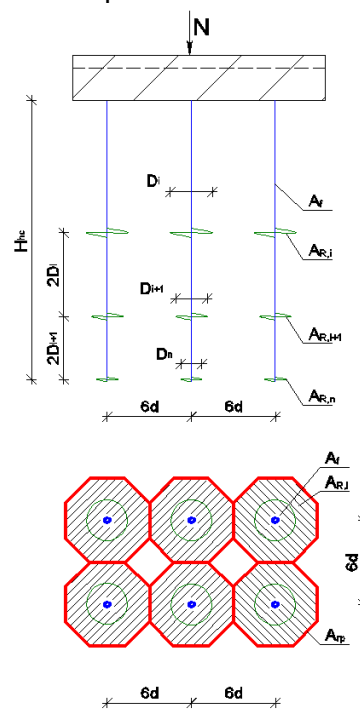


**Fig. 1 – Soil reinforcement scheme. A_f – shear surface of reinforcing element, $A_{R,i}$ – bottom bearing surface of reinforcing screw, d – vertical pipe's diameter, D_i – diameter of i screw, A_{Rp} – area of surrounding soil working mutually with reinforcing element
Image by the author of the article**

The installation of vertical reinforcing elements is intended to achieve joint resistance between the soil and the reinforcement. This joint action occurs when both components undergo equal and simultaneous deflections. Based on a review of existing approaches to settlement calculation in vertically reinforced weak soils, the following pre-design conditions are defined:

- specific geometry of helical shear screws;
- arrangement of vertical elements at a calculated spacing;
- the modulus of elasticity of the reinforcing elements is higher than that of the soil;
- shear extensions fabricated from materials stronger than the surrounding soil.

Shadunts K.Sh. emphasized the importance of considering the adhesion load required to ensure joint deformation of weak soil and reinforcing elements. Referring to Deryagin B.V. and Terzaghi K., he described this adhesion load as a molecular interaction between the two materials.

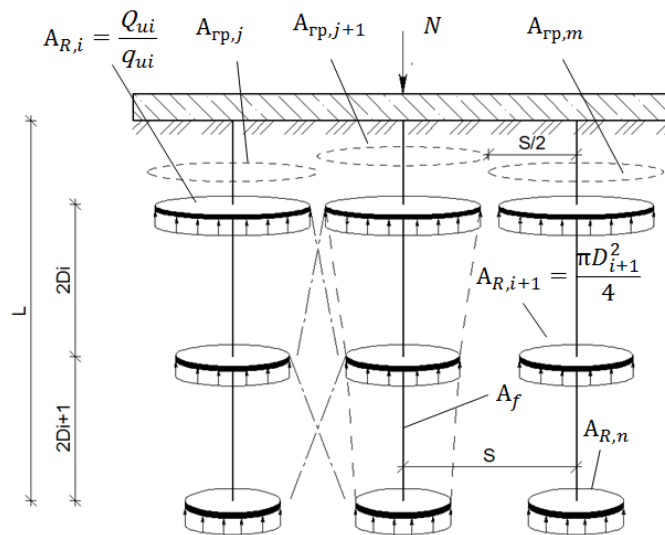


Fig. 2 – Reinforcing elements loading scheme
Image by the author of the article

2.2 Reinforcing element structure

The reinforcing elements consist of fiber-reinforced plastic (FRP) pipes with cast iron screws attached to the pipe surface. The FRP pipes are manufactured using the pultrusion method [34]. The screws are fixed to the pipe using adhesive or rivets. Their diameters increase progressively from the bottom toward the top of the element, while the spacing between adjacent screws is set equal to twice their diameter.

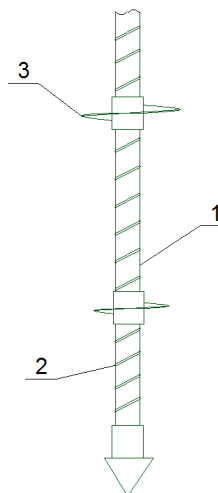


Fig. 3 – Multi screw type reinforcing element. 1 – fiber reinforced plastic pipe, 2 – spiral extra roving, 3 – screws
Image by the author of the article

A similar structure was previously developed by Svetlov L.P. It consisted of a micropile fabricated from an FRP pipe with a single screw located at the pile base, as later described by Nurmukhametov, R.R., and Mirsayapov, I.T. [35]. The disadvantage of this design was the requirement to install micropiles down to the underlying strong soil layer, which increased the consumption of FRP pipes and the complexity of the installation—the need for additional torque further complicated the process during driving. The higher rotation moment demanded greater pipe stiffness, as thin pipe walls tended to delaminate under excessive torque (Figure 4).



Fig. 4 – FRP delamination after oversized torque moment application
Image by the author of the article

Fiber-reinforced plastic (FRP) offers several advantages over traditional materials [36], [37], [38]. As a non-conductive material widely used for renovation [39] and regular structures reinforcement [40], FRP can be used as a foundation element for buildings and lightweight steel structures without risk of galvanic interaction [41]. Its electrical neutrality with soil prevents electrochemical corrosion of the reinforcement. Previous studies have also confirmed the benefits of composite materials for geotechnical applications [42].

A similar configuration was investigated by Boyarintcev A.V. [43], who designed a structure with smaller screw diameters for use in permanently frozen soils. However, this design is unsuitable for weak soils due to its low bearing capacity at the base.

The proposed soil reinforcement method can be applied to low-rise and demountable structures, owing to its rapid installation process. Due to its lightweight design, it is also suitable for northern regions and remote areas where transportation is challenging. The method is particularly applicable in road infrastructure and power supply construction.

2.3 Calculation method

The proposed approach is based on Terzaghi's theory of soil compaction and the experimental findings of Gersevanov N.M. In these studies, soil was modeled as an elastic porous material, while plastic deformations were incorporated through the factor of elastic–plastic deflections (ν).

The developed method considers uniaxial loading, where both the reinforcing elements and the surrounding soil deform simultaneously. Under external loading, the stress within the reinforced soil mass can therefore be expressed by the following equation:

$$\sigma_{a3}(\alpha) = \varepsilon_{a3} E_{a3} = \frac{\sigma_{rp}}{E'_{rp}} E_{a3} = \sigma_{rp} \alpha \frac{1}{\nu}, \quad (4)$$

Where:

$\alpha = \frac{E_{a3}}{E_{rp}}$ is the deformability factor, defined as the ratio of the reinforcement modulus of

deformability to the soil modulus of deformability;

ν – is the elastic–plastic deflection factor, defined as the ratio of elastic deflections to the total of elastic and plastic deflections

Considering static equilibrium, the external load is balanced by internal stresses within the reinforced soil element. The balance equation can be expressed as:

$$N = \sigma_{rp} A_{rp} + \sigma_{a3} A_{a3} = A_{rp} (\sigma_{rp} + \zeta_A \sigma_{a3}) = A_{rp} (\sigma_{rp} + \zeta_A \sigma_{rp} \frac{\alpha}{\nu}), \quad (5)$$

$$N = \sigma_{rp} A_{rp} \left(1 + \zeta_A \frac{\alpha}{\nu}\right), \tag{6}$$

Where ζ_A is the reinforcement factor, which defines the equivalent area of the reinforced soil mass and is given as:

$$\zeta_A = \frac{\gamma_{Frn} A_f + \gamma_{Rrn} A_{R,cp}}{A_{rp,cp}}, \tag{7}$$

Where:

A_f – shear surface area of the reinforcing element,

$A_{R,cp}$ – average bearing surface area of the reinforcing screws,

$A_{rp,cp}$ – area of surrounding soil acting jointly with the reinforcing element,

γ_{Frn} and γ_{Rrn} – reaction factors of shear and base surfaces, taken from nomograms (Figures 5 and 6). These nomograms, developed by Bartolomey A.A. and Antonov V.M., depend on the reinforcement spacing-to-length ratio, soil type (specifically, the clay fraction), and porosity factor.

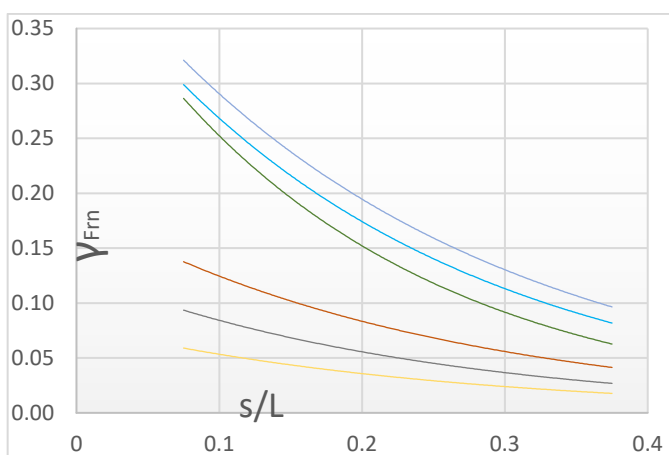


Figure 5 – shear surface reaction factor.

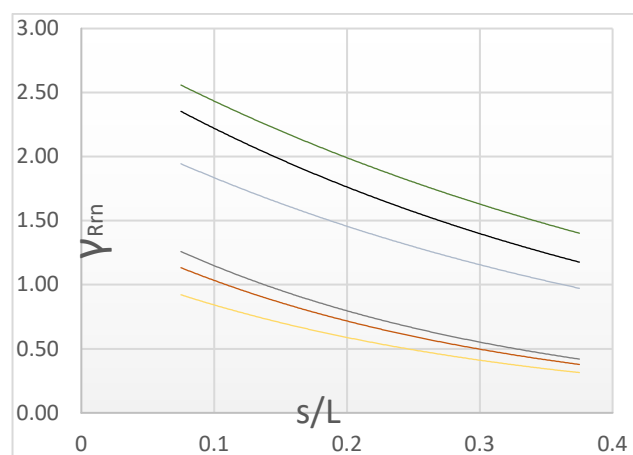


Figure 6 – bottom surface reaction factor.

The compressive stress in the reinforced soil can be defined as:

$$\sigma_{rp}(\zeta_A) = \frac{N}{A_{rp,cp} \left(1 + \zeta_A \frac{\alpha}{\nu}\right)}, \tag{8}$$

Where:

- N is the vertical applied load,
- $A_{rp,cp}$ is the average area of the surrounding soil acting jointly with the reinforcing element.

The average area is determined as:

$$A_{rp,cp} = \frac{\sum_{j=1}^m (A_{rp,j} + A_{rp,j+1})}{m}, \tag{9}$$

Substituting (9) into (8), the following relationship is obtained:

$$\sigma_{as} = \sigma_{rp} \frac{\alpha}{\nu} = \frac{\alpha N}{A_{rp}(\nu + \zeta_A \alpha)}, \tag{10}$$

Equation (10) was then applied in the framework of layer-by-layer settlement analysis. Thus, the settlement equation becomes:

$$S(\zeta_A) = m_{\nu} \int_0^{H_c} \sigma(z) dz = \sum_{i=0}^{H_c} h_i m_{\nu i} \sigma_{rpi}(\zeta_A) = \sum_{i=0}^{H_c} \frac{h_i m_{\nu i} N}{A_{rp,cp} \left(1 + \zeta_A \frac{\alpha}{\nu}\right)}, \tag{11}$$

In equation (11):

- m_v is the compaction factor,
- H_c is the settlement depth,
- $\sigma_{\rho i}$ is the stress in the i -th soil layer.

As a result, a settlement calculation formula was derived, accounting for the geometry, number, spacing, and screw diameters of the reinforcing elements.

2.4 Verification by site tests

Field tests were conducted to verify the proposed settlement calculation method. The reinforcement design was based on structural calculations for FRP pipes. Five types of reinforcing elements were fabricated (Figure 7):

- Element #1 – steel pipe,
- Element #2 – FRP pipe, 100 mm in diameter and 800 mm in length,
- Element #3 – FRP pipe, 75 mm in diameter and 2000 mm in length, with a single screw (300 mm diameter) at the base,
- Element #4 – FRP pipe identical to #3 but with an additional screw of the same diameter (300 mm) positioned 1200 mm above the bottom screw,
- Element #5 – FRP pipe identical to #3 and #4, but equipped with three screws of varying diameters: 150 mm, 225 mm, and 300 mm, arranged as shown in Figure 1.

All fiberglass and steel pipes had a uniform wall thickness of 4 mm.

The reinforcement elements were installed into the soil up to the ground surface and cut flush with it. A 200 mm thick sand bedding was placed above the reinforced soil to enable plate load tests. The tests were performed in accordance with GOST 20276.1-2020. Loading was applied to the soil reinforced with vertical elements using a hydraulic jack in increments of 0.6 kN. The applied load was measured by a manometer gauge and converted into force values generated by the jack.

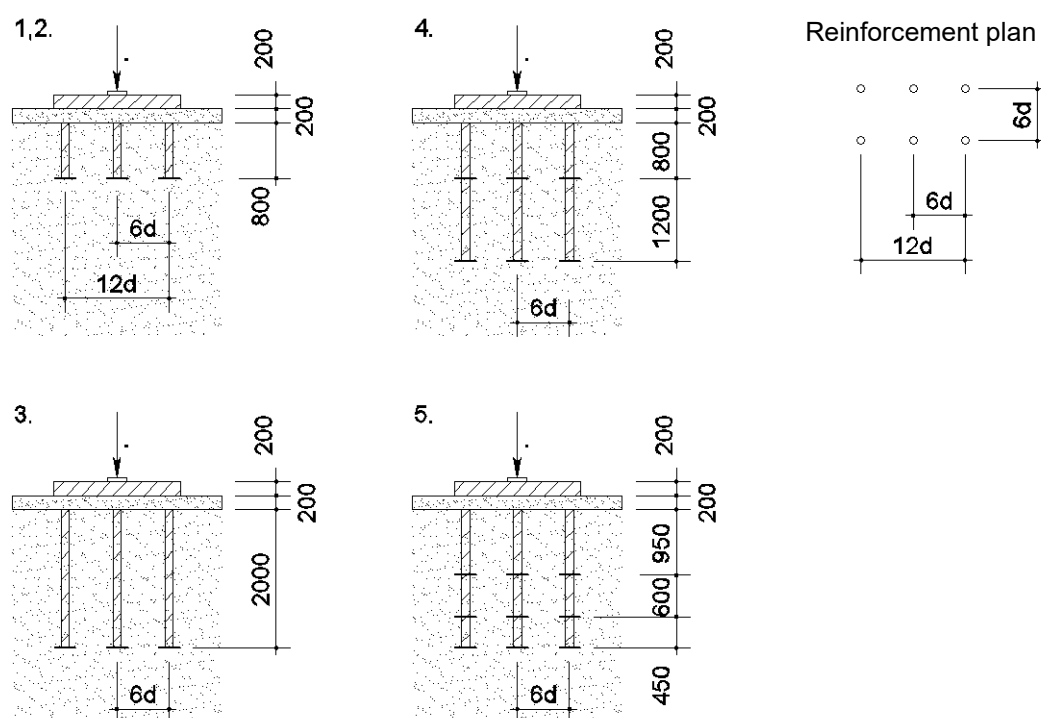


Fig. 7 – Scheme of performed site tests. 1 – reinforcement elements made with steel, $\zeta A = 0.23$, 2 – reinforcement elements made with fiberglass, diameter 100 mm, $\zeta A = 0.27$. 3 – reinforcement elements made with fiberglass diameter 75 mm, $\zeta A = 0.33$, 4 – reinforcement elements made with fiberglass diameter 75 mm with two screws, $\zeta A = 0.51$, 5 – reinforcement elements made with fiberglass diameter 75 mm with three different screws, $\zeta A = 0.72$

The load was applied through a 200 mm thick concrete slab placed on the sand bedding. The slab acted as a rigid plate, ensuring that the soil between the reinforcing elements was mobilized and allowing the reinforced soil mass to be evaluated as a single composite system. Additionally, the rigid slab allowed for the application of higher loads until the ultimate condition was reached.

3 Results and Discussion

Settlement measurements were obtained and verified during full-scale tests. The outcomes of these tests are presented in Figure 8.

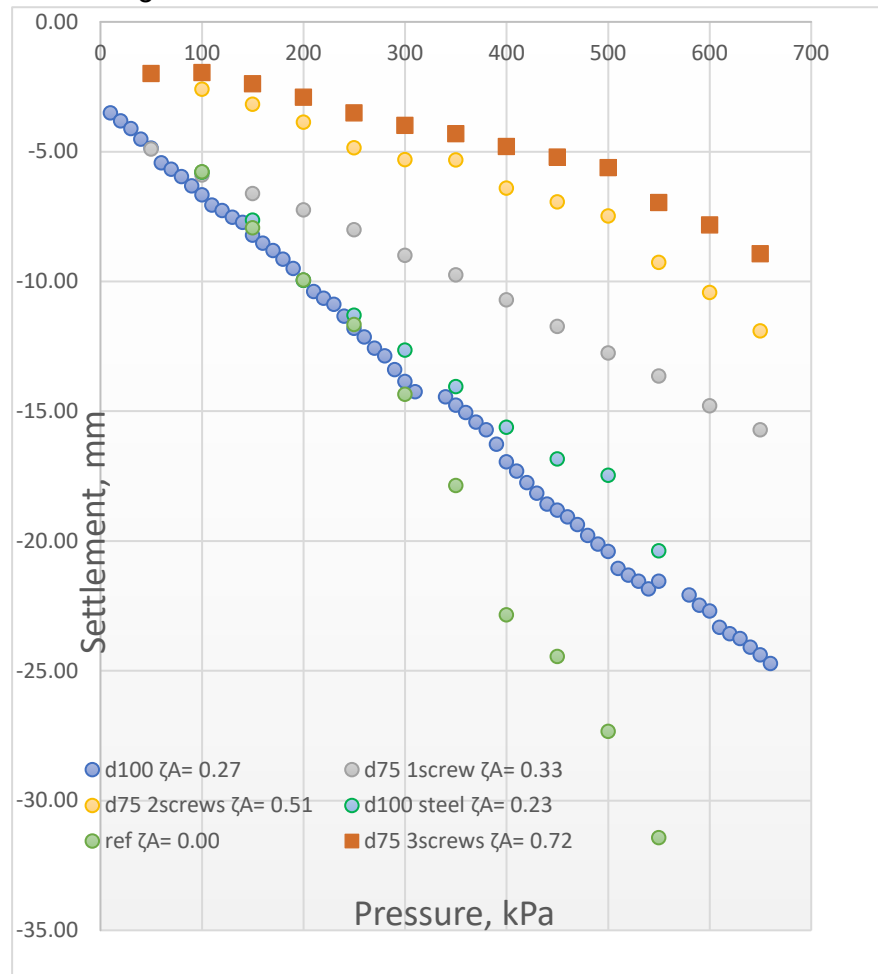


Fig. 8 – Load - settlement graphs of the tested samples before and after reinforcement

Comparison of test results demonstrates a reduction in vertical settlements with increasing reinforcement factor (ζ_A). For samples subjected to pressures below 400 kPa, low reinforcement rates ($\zeta_A = 0.23$ and 0.27) resulted in settlements that were 26–32% lower compared to non-reinforced samples.

A comparison of samples differing in installation depth revealed a 37% reduction in settlement under an applied pressure of 400 kPa. The compared samples had reinforcement factors $\zeta_A = 0.33$ and 0.27 , while the spacing between elements remained constant. These results confirm the hypothesis that reinforcement length directly influences the reinforcement factor, thereby increasing the rigidity of the reinforced soil.

Introducing a second and third screw in the middle section of the reinforcing element ($\zeta_A = 0.51$ and 0.72) further reduced settlements by 41% and 55%, respectively, compared with single-screw elements ($\zeta_A = 0.33$) under the same pressure of 400 kPa. The disproportionate increase in rigidity with multi-screw reinforcement indicates the contribution of the surrounding soil to composite behavior. Moreover, differentiated screw diameters reduced the effect of soil decompaction around the screws.

The measured vertical deflections confirmed the dependence of the reinforcement factor on both the ratio of screw diameters to their spacing and the spacing of reinforcing elements. Secant deformation moduli (E) were calculated for specific pressure levels (Table 1), using formulas prescribed by GOST 20276.1-2020.

Table 1. Influence of reinforcement factor on deflection module

	Reinforcement factor, ζ_A
--	---------------------------------

	0	0.23	0.27	0.33	0.51	0.72
Deflection module E, MPa	3.69	5.79	6.80	11.59	16.27	21.69

The deformation modulus obtained from the site tests (Figure 9) reflects the expected increase in soil rigidity due to reinforcement. The deformability of reinforced samples decreased compared with the unreinforced reference sample. The measured reductions were 3%, 12%, 37%, 63%, and 72% for reinforcement factors $\zeta_A = 0.23, 0.27, 0.33, 0.51,$ and $0.72,$ respectively. The comparison was performed under a constant applied pressure of 300 kPa.

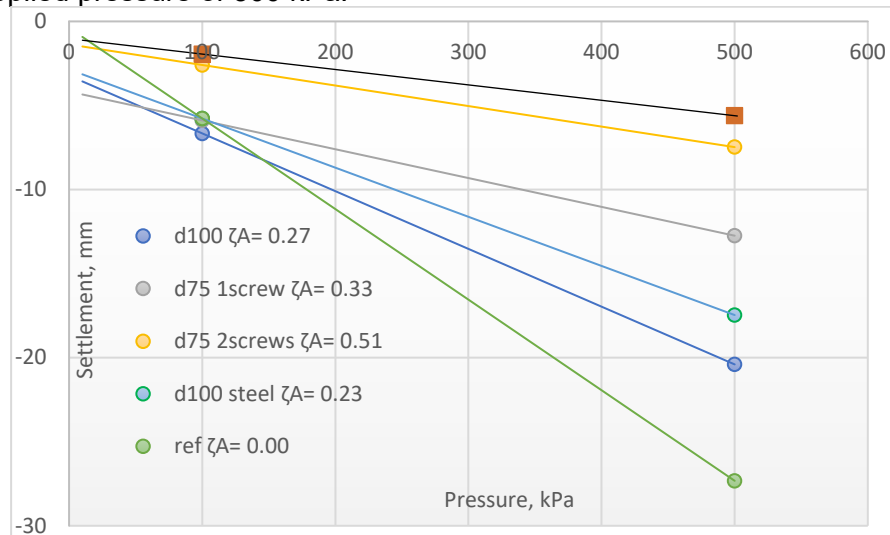


Fig. 9 – Graphs for deformation modules definition compared to reinforcement factor ζ_A

The results of the site tests are consistent with the laboratory experiments conducted earlier [44].

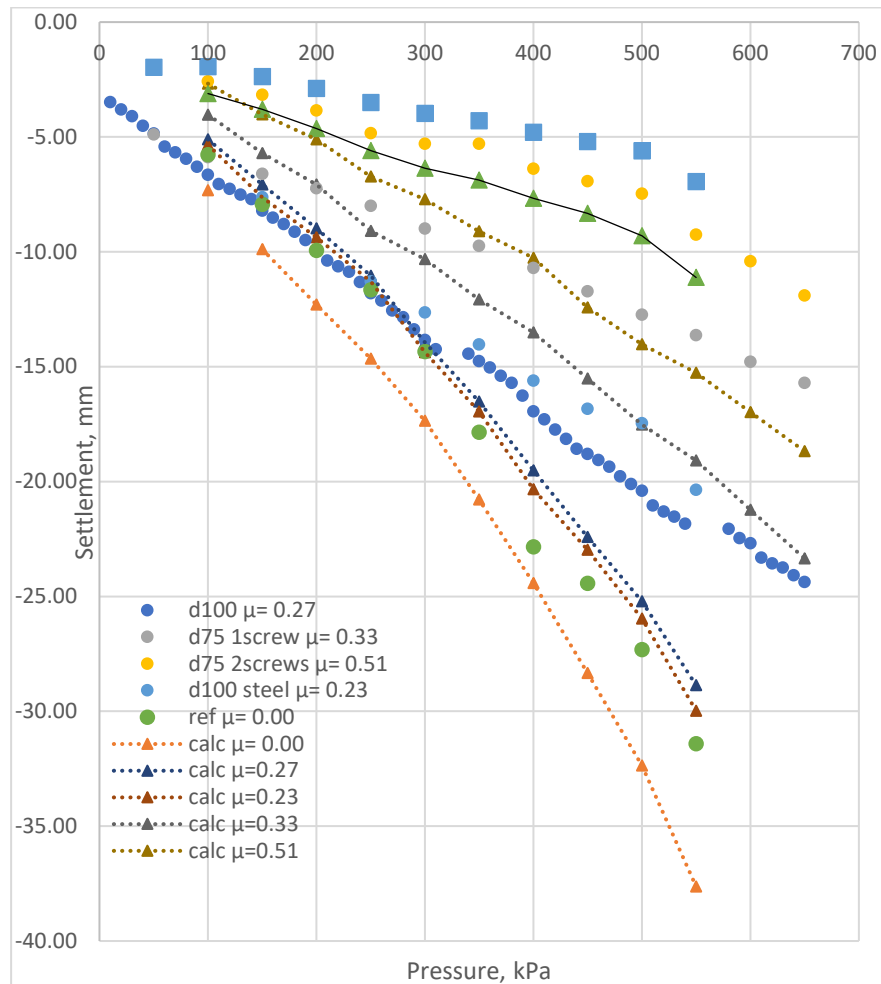


Fig. 10 – Test results compared to calculated results

Earlier test results by Mirsayapov I.T., Safin D.R., and Nurmukhametov R.R. [45], [46], [47] demonstrated that reinforcing elements act as boundaries that limit the deflections of weak soils.

4 Conclusions

Based on the theoretical analysis, the developed calculation method, and full-scale site tests, the following conclusions are drawn:

1. A revised scheme of weak soil reinforcement was proposed, employing vertical elements with screws of increasing diameters from bottom to top. This configuration mobilizes a larger soil volume while preserving its structure.
2. A settlement calculation method was developed, introducing a reinforcement factor that depends on the geometry and configuration of the reinforcing elements. The technique was adapted for FRP pipes with cast-iron screws.
3. The proposed method was validated through full-scale tests, confirming its applicability for predicting settlements in reinforced soils.
4. The designed multi-screw reinforcing elements demonstrated significant efficiency. Under an applied pressure of 300 kPa, settlement reductions of 63% (two screws) and 72% (three screws) were achieved compared with the unreinforced reference sample.
5. The findings provide both theoretical and experimental justification for applying FRP-based multi-screw reinforcement in weak soils, particularly for low-rise buildings, temporary structures, and infrastructure in regions with difficult access.

References



- 1 Yuan, C., Hao, D., Ding, S. and Ding, M. (2024) Field Experimental Study on the Uplift and Lateral Capacity of Deep Helical Anchors and Grouped Helical Anchors in Clays. *Buildings*, **14**, 662. <https://doi.org/10.3390/BUILDINGS14030662>
- 2 Yang, T., Zheng, W., Xie, Y., Zhang, H. and Yue, X. (2023) Evaluating Screw-Shaft Pile Composite Foundations in Round Gravelly Soil: A Study Using Model Tests and Numerical Simulations. *Heliyon*, **9**. <https://doi.org/10.1016/J.HELIYON.2023.E20887>
- 3 Nurmukhametov, R.R. (2019) Reduction of Water Saturated Clayey Soils' Deflections by Reinforcement. *Construction of Unique Buildings and Structures*, **9**, 22–33. <https://doi.org/10.18720/CUBS.84.2>
- 4 Zhao, C., Xu, C., Shen, P., Li, G. and Wang, Q. (2024) Assessing Numerical Simulation Methods for Reinforcement–Soil/Block Interactions in Geosynthetic-Reinforced Soil Structures. *Buildings*, **14**, 422. <https://doi.org/10.3390/BUILDINGS14020422>
- 5 Maltseva, T., Nabokov, A., Novikov, Y. and Sokolov, V. (2016) The Method of Calculating the Settlement of Weak Ground Strengthened with the Reinforced Sandy Piles. *MATEC Web of Conferences, EDP Sciences*. <https://doi.org/10.1051/mateconf/20167301015>
- 6 Chaplin, I. and Yashnov, A. (2018) Specifics of Determining the Tension Forces of the Cable-Stayed Bridge Elements. *MATEC Web of Conferences*, 05011. <https://doi.org/10.1051/mateconf/201823905011>
- 7 Zasukhin, I., Ivanov, A., Kuzmenkov, P., Polyakov, S. and Chaplin, I. (2023) Features of Bridge Superstructures Modeling during the Stress-Strain State Monitoring. *E3S Web of Conferences*, 10030. <https://doi.org/10.1051/e3sconf/202346010030>
- 8 Khan, A.R. and Di Emidio, G. (2025) Reinforced Fill Structure with Alternative Fill Materials: An Application of Geogrid Creep Strain Analysis Using Numerical Modeling. *Materials, Multidisciplinary Digital Publishing Institute (MDPI)*, **18**, 1346. <https://doi.org/10.3390/MA18061346>
- 9 Phan, T.T.T., Gui, M.W., Pham, T. and Luong, B.T. (2025) Numerical Analysis of the Stress–Deformation Behavior of Soil–Geosynthetic Composite (SGC) Masses Under Confining Pressure Conditions. *Buildings*, **15**, 2229. <https://doi.org/10.3390/BUILDINGS15132229>
- 10 Rahmaninezhad, S.M., Han, J. and Al-Naddaf, M. (2020) Limit Equilibrium Analysis of Geosynthetic-Reinforced Retaining Walls Subjected to Footing Loading. *American Society of Civil Engineers*, 464–471. <https://doi.org/10.1061/9780784482797.045>
- 11 Zeng, J.-J., Hao, Z.-H., Jiang, Y.-Y., Liang, Q.-J., Liu, Y. and Zhuge, Y. (2024) Long-Term Durability of UHPECC-Embedded GFRP Bars in Alkaline Environments. *Journal of Composites for Construction, American Society of Civil Engineers (ASCE)*, **28**, 04024065. <https://doi.org/10.1061/JCCOF2.CCENG-4834>
- 12 Bartolomey, A.A., Kleveko, V.I., Ofrikhter, V.G., Ponomaryov, A.B. and Bogomolov, A.N. (1999) The Use of Synthetic Materials in the Highway Engineering in the Urals. *Geotechnical Engineering for Transportation Infrastructure. Proceedings of the 12th European Conference on Soil Mechanics and Geotechnical Engineering*, **2**, 1197–1202. <https://trid.trb.org/view/638112>
- 13 García-Aristizábal, E.F., Vega-Posada, C.A. and Gallego-Hernández, A.N. (2016) Experimental Study of Water Infiltration on an Unsaturated Soil-Geosynthetic System. *Revista Facultad de Ingeniería*, **2016**, 112–118. <https://doi.org/10.17533/udea.redin.n78a15>
- 14 Das, B. and Chetia, N. (2020) Experimental Studies on Load Settlement Behavior of Cohesion Less Soil Using Bamboo. *International Journal of Advanced Engineering Research and Science*, **7**, 45–49. <https://doi.org/10.22161/ijaers.74.5>
- 15 Tatar, J. and Milev, S. (2021) Durability of Externally Bonded Fiber-Reinforced Polymer Composites in Concrete Structures: A Critical Review. *Polymers*, **13**, 765. <https://doi.org/10.3390/POLYM13050765>
- 16 Yu, X., Wu, X., Zhu, P., Liu, C., Qiu, C. and Cai, Z. (2025) Mechanism of Strength Degradation of Fiber-Reinforced Soil Under Freeze–Thaw Conditions. *Buildings*, **15**, 842. <https://doi.org/10.3390/BUILDINGS15060842>
- 17 Igosheva, L. and Grishina, A. (2016) Design of Experiments to Consolidate the Water-Saturated Clay Soil Base by Magnesium Sulfate in the Construction of Buildings and Structures. *PNRPU Construction and Architecture Bulletin*, **7**, 102–110. <https://doi.org/10.15593/2224-9826/2016.4.10>
- 18 Igosheva, L.A. and Grishina, A.S. (2016) Review of the Basic Methods of the Ground Improvement. *PNRPU Bulletin Construction and Architecture*, **7**, 5–21. <https://doi.org/10.15593/2224-9826/2016.2.01>

Nurmukhametov R.

Multi screw type elements for weak soil reinforcement;
2025; *AlfaBuild*; **34** Article No 3404. doi: 10.57728/ALF.34.4



- 19 Sabri, M.M. and Shashkin, K.G. (2020) Subsoil Stabilized by Polyurethane Resin Injection: FEM Calculation. *Construction of Unique Buildings and Structures*, **98**. <https://doi.org/10.18720/CUBS.91.8>
- 20 Sabri, M.M.S. and Shashkin, K.G. (2020) The Mechanical Properties of the Expandable Polyurethane Resin Based on Its Volumetric Expansion Nature. *Magazine of Civil Engineering*, **98**. <https://doi.org/10.18720/MCE.98.11>
- 21 Kudryavtsev, S., Valtseva, T., Bugunov, S., Kotenko, Z., Paramonov, V., Saharov, I. and Sokolova, N. (2020) Numerical Simulation of the Work of a Low-Settlement Embankment on a Pile Foundation in the Process of Permafrost Soil Thawing. *Lecture Notes in Civil Engineering*, 73–82. https://doi.org/10.1007/978-981-15-0454-9_9
- 22 Sokolov, V.A., Strakhov, D.A., Sinyakov, L.N. and Garmanov, G. V. (2017) Effectiveness of Jet Grouting Method for Soil Base Strengthening. *Construction of Unique Buildings and Structures*, **56**, 63. <https://doi.org/10.18720/CUBS.56.5>
- 23 Sabri M.M., Shashkin, K.G., Zakharin, E. and Ulybin, A.V. (2018) Soil Stabilization and Foundation Restoration Using an Expandable Polyurethane Resin. *Magazine of Civil Engineering*, **82**, 68–80. <https://doi.org/10.18720/MCE.82.7>
- 24 Sabri, M.M. and Shashkin, K.G. (2018) Improvement of the Soil Deformation Modulus Using an Expandable Polyurethane Resin. *Magazine of Civil Engineering*, **83**, 222–234. <https://doi.org/10.18720/MCE.83.20>
- 25 Popov, A.O. (2015) Settlement Calculation of Clay Bed Reinforced with Vertical Elements. *Magazine of Civil Engineering*, St-Petersburg State Polytechnical University, **56**. <https://doi.org/10.5862/MCE.56.3>
- 26 Mirsayapov, I.T. and Koroleva, I. V. (2011) Prediction of Deformations of Foundation Beds with a Consideration of Long-Term Nonlinear Soil Deformation. *Soil Mechanics and Foundation Engineering*, **48**, 148–157. <https://doi.org/10.1007/s11204-011-9142-8>
- 27 Zahmatkesh, A. and Choobbasti, A.J. (2012) Settlement Evaluation of Soft Clay Reinforced with Stone Columns Using the Equivalent Secant Modulus. *Arabian Journal of Geosciences*, **5**, 103–109. <https://doi.org/10.1007/s12517-010-0145-y>
- 28 Poorooshasb, H. and Meyerhof, G. (1996) Analysis of Behavior of Stone Columns and Lime Columns. *Comput Geotech*, **20**, 47–70. [https://doi.org/10.1016/S0266-352X\(96\)00013-4](https://doi.org/10.1016/S0266-352X(96)00013-4)
- 29 Alnmr, A., Ray, R.P., Alsirawan, R., Yang, H.-W., Wang, S., Cao, C., Alnmr, A., Ray, R.P. and Alsirawan, R. (2023) A State-of-the-Art Review and Numerical Study of Reinforced Expansive Soil with Granular Anchor Piles and Helical Piles. *Sustainability*, **15**, 2802. <https://doi.org/10.3390/SU15032802>
30. Francisco Mayuet Ares, P., Sampaio, Á., De la Rosa Silva, S., Kim, S.-H., Joo, H.-J. and Choi, W. (2024) Structural Behavior of High Durability FRP Helical Screw Piles Installed in Reclaimed Saline Land. *Polymers*, **16**, 1733. <https://doi.org/10.3390/POLYM16121733>
- 31 Khalid, B., Alshawmar, F., Khalid, B. and Alshawmar, F. (2024) Comprehensive Review of Geotechnical Engineering Properties of Recycled Polyethylene Terephthalate Fibers and Strips for Soil Stabilization. *Polymers*, **16**, 1764. <https://doi.org/10.3390/POLYM16131764>
- 32 Zhao, H., Tserpes, K., Belouettar, S., Mofidi, A. and Rajabifard, M. (2025) Fracture Mechanics-Based Modelling of Post-Installed Adhesive FRP Composite Anchors in Structural Concrete Applications. *Journal of Composites Science*, **9**, 282. <https://doi.org/10.3390/JCS9060282>
- 33 Abdelghany, Y., El Naggat, M.H., Abdelghany, Y., Hesham, M., Naggat, E. and Naggat, H. El. (2014) Full-Scale Field Investigations and Numerical Analyses of Innovative Seismic Composite Fiber-Reinforced Polymer and Reinforced Grouted Helical Screw Instrumented Piles Under Axial and Lateral Monotonic and Cyclic Loadings. *Advances in Soil Dynamics and Foundation Engineering*. <https://doi.org/10.1061/9780784413425.042>
- 34 Malikov, D.A., Vasyutkin, E.S., Burin, D.L.; Dzhahalov, A.I., Ismailov, A.M., Kovalev, M.A., Tokarev, V.O. and Birryukov, D.V. (2021) Durability and Performance of Composite Pipes Under Conditions of Exposure to High Temperatures of the Transported Liquid. *AlfaBuild*, **3(18)**, 1805-1805. <https://alfabuild.spbstu.ru/article/2021.18.5/>
- 35 Nurmukhametov, R.R., Vatin, N.I., Mirsayapov, I.T., Vasyutkin, E.S., Burin, D.L. and Vasyutkin, S.F. (2020) FRP Helical Micro Screw Pile with Cast Iron Pile Cap: Review. *Construction of Unique Buildings and Structures*, **89**, 8903. <https://doi.org/10.18720/CUBS.89.3>



- 36 Salakhutdinov, M.A., Gimranov, L.R., Kuznetsov, I.L., Fakhrutdinov, A.E. and Nurgaleeva, L.M. (2020) PFRP Structures under the Predominately Short Term Load. *Magazine of Civil Engineering*, **96**, 3–14. <https://doi.org/10.18720/MCE.96.1>
- 37 Pinyazhin, S., Ivanov, A., Yashnov, A. and Ermolov, Y. Structural Solutions of the Superstructure with Elements Made of Polymer Composite Material. *Proceedings of the II International Scientific Conference on Advances in Science, Engineering and Digital Education*, 1–10. <https://doi.org/10.1063/5.0118648>
- 38 Biryukov, D. V., Denisov, V.N. and Schwartz, M.S. (2017) Protection of Structures from Moisture as a Priority for the Preservation of Buildings and Structures. *Bulletin of Civil Engineers*, **1**, 127–134. <https://vestnik.spbgasu.ru/en/article/protection-structures-humidification-priority-direction-buildings-and-facilities>
- 39 Veber, M.D. and Kuznetsov, A. V. (2025) On Restoring Cantilever Stone Staircases in the Architecture of St. Petersburg. Part 1. <https://doi.org/10.20295/1815-588X-2025-2-509-530>
- 40 Kurlapov, D., Klyuev, S., Biryukov, Y., Vatin, N., Biryukov, D., Fediuk, R. and Vasilev, Y. (2021) Reinforcement of Flexural Members with Basalt Fiber Mortar. *Fibers*, **9(4)**, 26. <https://doi.org/10.3390/fib9040026>
- 41 Garifullin, M., Bronzova, M.K., Heinisuo, M., Mela, K. and Pajunen, S. (2018) Cold-Formed {RHS} {T} Joints with Initial Geometrical Imperfections. *Magazine of Civil Engineering*, **80**, 81–94. <https://doi.org/10.18720/MCE.80.8>
- 42 Wang, W., Cheng, Y., Chen, H. and Tan, G. (2023) Polymeric Composites in Road and Bridge Engineering: Characterization, Production and Application. *Polymers*, **15(4)**, 874. <https://doi.org/10.3390/polym15040874>
- 43 Boyarintsev, A. V. (2020) Polymer and Composite Piles. International and Russian Experience. *Soil Mechanics and Foundation Engineering*, **57**, 415–421. <https://doi.org/10.1007/s11204-020-09686-9>
- 44 Sabri, M.M.S., Vatin, N.I., Nurmukhametov, R.R., Ponomarev, A.B. and Galushko, M.M. (2022) Vertical Fiberglass Micropiles as Soil-Reinforcing Elements. *Materials*, **15**. <https://doi.org/10.3390/ma15072592>
- 45 Mirsayapov, I., Nurmukhametov, R., Vasyutkin, E. and Burin, D. (2021) FEA Analysis of Fiberglass Piles' Bearing Capacity at Water Saturated Soft Clay. *Proceedings of EECE 2020*. https://doi.org/10.1007/978-3-030-72404-7_38
- 46 Nurmukhametov, R.R. (2019) Deformability of Water Saturated Clay Reinforced by Vertical Elements. *Alfabuild*, **4**, 54–69. <https://doi.org/10.6084/m9.figshare.11637849>
- 47 Safin, D.R. (2008) Study of Deformability of Vertically Reinforced Water-Saturated Argillir Soil Bodies. *Kazan State University of Architecture and Engineering (KSUAE)*, **2**, 81–84. https://izvestija.kgasu.ru/ru/nomera-zhernala/arkhiv-zhurnalala?sod=sod2_2008&idizv=45